

Ventilation Rates Estimated from Tracers in the Presence of Mixing

TIMOTHY M. HALL,* THOMAS W. N. HAINE,⁺ MARK HOLZER,[#] DEBORAH A. LEBEL,[@]
FRANCESCA TERENCE,[#] AND DARRYN W. WAUGH⁺

**NASA Goddard Institute for Space Studies, New York, New York*

⁺ Department of Earth and Planetary Sciences, The Johns Hopkins University, Baltimore, Maryland

[#] Department of Applied Physics and Applied Mathematics, Columbia University, New York, New York

[@] Lamont-Doherty Earth Observatory, Columbia University, Palisades, New York

(Manuscript received 11 October 2005, in final form 4 December 2006)

ABSTRACT

The intimate relationship among ventilation, transit-time distributions, and transient tracer budgets is analyzed. To characterize the advective–diffusive transport from the mixed layer to the interior ocean in terms of flux we employ a cumulative ventilation-rate distribution, $\Phi(\tau)$, defined as the one-way mass flux of water that resides at least time τ in the interior before returning. A one-way (or gross) flux contrasts with the net advective flux, often called the subduction rate, which does not accommodate the effects of mixing, and it contrasts with the formation rate, which depends only on the net effects of advection and diffusive mixing. As τ decreases $\Phi(\tau)$ increases, encompassing progressively more one-way flux. In general, Φ is a rapidly varying function of τ (it diverges at small τ), and there is no single residence time at which Φ can be evaluated to fully summarize the advective–diffusive flux. To reconcile discrepancies between estimates of formation rates in a recent GCM study, $\Phi(\tau)$ is used. Then chlorofluorocarbon data are used to bound $\Phi(\tau)$ for Subtropical Mode Water and Labrador Sea Water in the North Atlantic Ocean. The authors show that the neglect of diffusive mixing leads to spurious behavior, such as apparent time dependence in the formation, even when transport is steady.

1. Introduction

The transport of water and trace constituents between the ocean's seasonal mixed layer and the permanently stratified interior sets the temperature, salinity, and trace-gas composition for much of the ocean. Quantifying this transport is crucial for understanding the ocean's role in climate, and there has been intense interest for many years in estimating these fluxes. The paucity of observations, however, prevents the direct calculation of fluxes across the mixed layer base from fluid velocities, although such calculations have been performed on highly smoothed observational datasets (Marshall et al. 1993, 1998) and on GCM data (Hazeleger and Drijfhout 2000). Transient tracers offer an attractive alternative. Tracers sample all the transport pathways from the surface to interior. These pathways include the direct trajectories as well as the meandering

trajectories whose pseudorandomness is due to both resolved and unresolved eddies and whose aggregate effect is diffusive. (Throughout, we use the word “transport” generally to include both bulk advection and eddy–diffusive mixing.) If a tracer is transient, then it has a nonzero rate of change of inventory from which a flux can be estimated.

A natural approach in tracer analysis is to relate the tracer's mass, $I(t)$, in some approximately closed domain (e.g., a region of the ocean interior defined by isopycnal surfaces and the mixed layer base) to the tracer's mole fraction history, $C_0(t)$, on the boundary of the formation region of the domain, that is, the domain's mixed layer base. If the transport occurs strictly in one direction from the formation region into the domain's interior and there are no other sources or sinks, then the relationship is particularly simple: The tracer mass flux (mass/time) is $\rho RC_0(t)$, where ρ is the water density and R is the volume flux (volume/time) of water across the mixed layer base. Here R is often termed the formation rate. (We discuss terminology in more detail below.) The tracer mass, or “inventory,” is obtained by accumulating the flux over time:

Corresponding author address: T. M. Hall, NASA Goddard Institute for Space Studies, 2880 Broadway, New York, NY 10025.
E-mail: thall@giss.nasa.gov

$$I(t) = \rho \int_{t_0}^t R(t') C_0(t') dt'. \quad (1)$$

If the transport is steady, then the volume flux R comes out of the integral. Given estimates of I and C_0 and a water-mass density ρ , one can then estimate R subject to the assumptions that go into expression (1).

Variants of (1) have been applied to chlorofluorocarbons (CFC) measurements in several studies. Smethie and Fine (2001) estimated a formation rate of 7.4 Sv (Sv $\equiv 10^6 \text{ m}^3 \text{ s}^{-1}$) for Labrador Sea Water (LSW), Rhein et al. (2002) estimated a formation rate of 4.4–5.6 Sv for LSW, and Orsi et al. (1999) estimated the formation rate of 12 Sv for Antarctic Bottom Water (AABW). Details of these analyses differ, and the investigators have estimated sensitivities to several assumptions. Smethie and Fine (2001) and Rhein et al. (2002) estimate the effects of variable transport, obtaining wide differences in formation rates in years of weak and strong LSW convection. Rhein et al. (2002) compare the vertical structure in the Labrador Sea before and after formative convective events, and thus, in contrast to Smethie and Fine (2001), their estimated rate encompasses formation within the Labrador Sea itself. Kieke et al. (2006) estimate upper LSW formation rates by differencing CFC inventories estimated from different years. Orsi et al. (1999) estimate limits on the rate at which CFCs are transferred across upper and lower AABW boundaries in the interior.

These analyses have highlighted the great utility of transient tracers in the diagnosis of ocean transport, and the investigators have carefully addressed many of the uncertainties. However, a key assumption implicit in relationship (1) is made in all of the analyses, namely, that the transport of water across the winter mixed layer base occurs strictly in one direction. Such a situation can only arise if mixing is a negligible component of transport, an assumption which is often suspect. A number of studies have demonstrated important roles for isopycnal mixing (e.g., Robbins et al. 2000). In the presence of mixing there is flux in both directions across a surface. In a GCM study Haine et al. (2003) observed that 60% of the Subpolar Mode Water (SPMW) that formed in the Labrador and Irminger Seas returned to the deep winter mixed layer in these seas within 8 years. One could accept relationship (1) as defining a formation rate R , but this leads to unappealing features in the presence of mixing between the formation region and interior of a water mass. So defined, R depends on the particular tracer and varies in time with the tracer history, even if the underlying transport is steady.

Our goal is to develop and illustrate a tracer-inde-

pendent flux diagnostic that includes the effects of mixing at all scales. To this end we consider a diffusive component of transport because diffusion captures the effects on tracers and water of the eddy-induced fluxes in both directions across the mixed layer base. Even though the net flux may be zero, the opposing one-way, or gross, fluxes are nonzero, causing an exchange of water and tracer. In fact, in the continuum fluid limit of an advective–diffusive flow the gross fluxes are infinite (Hall and Holzer 2003; Primeau and Holzer 2006). Conditions on the flux must be imposed, such as a minimum threshold of residence time in the interior, in order that the flux usefully diagnose transport. Generally, the conditioned flux will vary strongly with the threshold and should be considered as a function of the threshold. In this context, a single, finite value of flux derived from a tracer without explicit, controlled conditioning is difficult to interpret.

In addition to estimating ventilation rates, transient tracers have been used to determine the “age” of water parcels. Traditionally, this age is taken to be the time since the water parcel was last at the surface. Much recent work has highlighted the fact that, due to mixing, there is no unique transit time (age) from the surface to the water parcel position, even for a single surface-source region (e.g., Beining and Roether 1996; Deleersnijder et al. 2001; Haine and Hall 2002; Waugh et al. 2003; Primeau 2005). Instead, one must consider a transit-time distribution (TTD), which is a probability density function (PDF) of transit times. A transient tracer provides a constraint on the TTD, but alone cannot completely characterize it.

In this paper we explore the intimate connection among ventilation rate, TTDs, and transient tracer budgets. We show that, just as no single transit time can characterize the history of a water parcel’s last contact with the surface, no single value of flux can characterize the ventilation of the domain containing the parcel. As an alternative we advocate a “cumulative ventilation-rate distribution,” $\Phi(\tau)$, namely, the flux into the domain of water mass that resides at least τ in the domain before exiting across the same surface. For steady-state transport $\Phi(\tau)$ is equal to the integral of the TTD over the domain mass and it is closely related to the TTD for time-varying transport. The total flux $\Phi(0)$ (the one-way, or “gross,” flux of water mass that resides any length of time at all) is infinite in the continuum fluid limit for nonzero diffusivity. The total one-way flux is completely dominated by small-scale, unresolved, back-and-forth motions across the base of the mixed layer and is not, therefore, a useful diagnostic of the transfer. In contrast, the distribution, $\Phi(\tau)$, is integrable, finite at

finite τ , and characterizes the flux into the domain and, equivalently (in steady state), the age structure within the domain.

We first discuss general properties of the cumulative ventilation-rate distribution. Subsequently, we employ the cumulative ventilation-rate distribution to reconcile differences between GCM ventilation rates estimated by Haine et al. (2003) using two different tracers. We then apply a statistical model to bound $\Phi(\tau)$ for Subtropical Mode Water (STMW) and LSW in the North Atlantic Ocean using World Ocean Circulation Experiment (WOCE) CFC11 data. Last, we contrast this new ventilation diagnostic with other tracer-based approaches to estimating water fluxes.

2. Generalized ventilation

a. Nomenclature: Formation, subduction, and ventilation

We aim to diagnose the advective–diffusive transport of water one way across a fixed surface that divides the volume of an isopycnal water mass into a seasonal mixed layer, in which air–sea exchange occurs, and an interior. By “one way” we mean a gross flux, in contrast to a net flux that is in general the difference of opposing gross fluxes. The task is distinct from the estimates of formation and subduction rates of net volume flux supplying interior water masses. The formation rate is the tendency of the volume of a density class due to buoyancy fluxes at the sea surface. A fraction of these changes is reversible due to seasonality in the mixed layer depth. The remainder is balanced, in an annually averaged steady state, by a net volume flux (advective and diffusive) out through the base of the winter mixed layer. Such formation rates have been estimated thermodynamically by analysis of temperature and salinity air–sea exchange (Walsh 1982; Speer and Tziperman 1992; Marsh 2000). Formation rates are related to subduction rates, which are fluxes estimated kinematically by analysis of Ekman pumping and fluid velocity components on the mixed layer base (Marshall et al. 1993, 1998). Volume fluxes through the mixed layer base have also been estimated from the budgets of transient tracers, and these fluxes have been termed formation rates (Orsi et al. 1999; Smethie and Fine 2001; Rhein et al. 2002). As we argue below, however, in cases in which eddy mixing plays an important role in transporting tracer between the formation region and interior of a water mass the tracer-based flux estimates are equivalent to neither the thermodynamic formation rate nor the kinematic subduction rates and, indeed, are dependent on the particular tracer employed.

The subduction rate and formation rate are valuable

diagnostics of ocean circulation and density structure, but they are incomplete summaries of the advective–diffusive transport of water properties. The subduction rate is a net advective flux across the mixed layer base, while water properties are propagated in part by diffusive mixing, which arises from the pseudorandom motions induced by eddy structures in the flow field at both resolved and unresolved scales. By water “properties” we mean not only the concentrations of trace constituents, such as CFCs and dissolved carbon, but also labels such as the “region of last surface contact” and “elapsed time since last surface contact,” which are effectively tracers. Advective–diffusive transport occurs even when the net volume flux is zero. Corrections to the subduction rate by inclusion of a bolus velocity derived from eddy fluctuations alter the net advective flux, but cannot represent the diffusive effects of eddy mixing. In contrast to the subduction rate the formation rate is sensitive to diffusive mixing because the buoyancy budget in the mixed layer depends on the net diffusive transport of buoyancy across the mixed layer base (Marshall et al. 1998). However, a tracer-independent gross diffusive flux into the interior cannot readily be isolated from the other terms contributing to the buoyancy budget.

Our primary goal is to complement the formation and subduction rate diagnostics by developing and applying a tracer-independent gross flux diagnostic through the mixed layer base that includes the diffusive effects of mixing. To distinguish this flux from formation and subduction rates, and to be consistent with the terminology of Primeau and Holzer (2006), we refer to it as a ventilation rate. In much of our analysis we assume the transport to be in steady state, although this is not formally required. The formal development of our ventilation diagnostic (most of which is contained in the appendix) is general and does not depend on any particular model for the circulation. However, we subsequently apply the concepts to GCM data and to observational data using a simple low-parameter statistical model.

b. Green functions

Implicit in any relationship between the inventory of a tracer in a domain and the mole fraction history of the tracer in the domain’s formation region (e.g., the mixed layer base) is a transport Green function, or boundary propagator, that propagates the known mole fraction boundary condition into the domain. Given a spatially uniform boundary condition on tracer mole fraction, $C_0(t)$, on the edge of the domain’s formation region, the concentration at an interior point \mathbf{r} is

$$C(\mathbf{r}, t) = \int_{t_0}^t C_0(t') \mathcal{G}(\mathbf{r}, t, t') dt', \quad (2)$$

where $\mathcal{G}(\mathbf{r}, t, t')$ is a boundary propagator (units 1/time) that carries information on the boundary at time t' to location \mathbf{r} at time t . If the transport is in steady state, then \mathcal{G} depends on t and t' only through their difference $\tau \equiv t - t'$ (termed transit time), and we have, after a change of variables,

$$C(\mathbf{r}, t) = \int_0^\infty C_0(t - \xi) \mathcal{G}(\mathbf{r}, \tau) d\tau. \quad (3)$$

Here $\mathcal{G}(\mathbf{r}, \tau)$ has the physical interpretation as a TTD for water to reach \mathbf{r} from the boundary (Holzer and Hall 2000; Haine and Hall 2002). For pure one-dimensional bulk advection from x_0 to x at speed u one has $\mathcal{G}(x, \tau) = \delta[\tau - (x - x_0)/u]$, that is, a delta function at the transit time $(x - x_0)/u$. Many studies, however, have deduced a large role for isopycnal mixing (e.g., Jenkins 1988; Robbins et al. 2000), which gives rise to a range of transit times from the mixed layer to \mathbf{r} . In fact, the TTD have been found to be broad and asymmetric in GCM studies (Khaliwala et al. 2001; Haine and Hall 2002; Primeau 2005) and in observational analyses (Waugh et al. 2004). Integrating both sides of Eq. (3) over the domain of volume V and uniform density ρ (i.e., an isopycnal volume) yields the tracer inventory

$$I(t) = V\rho \int_0^\infty C_0(t - \xi) \bar{\mathcal{G}}(\tau) d\tau, \quad (4)$$

where

$$\bar{\mathcal{G}}(\tau) \equiv \frac{1}{V} \int_V d^3r \mathcal{G}(\mathbf{r}, \tau)$$

is the domain-averaged transit-time distribution, with the interpretation that $\bar{\mathcal{G}}(\tau) \delta\tau$ is the mass fraction of water in V that was last at the boundary a time τ to $\tau + \delta\tau$ ago. An analogous expression defines $\bar{\mathcal{G}}(t, t')$ in the more general case of time-varying transport.

c. The cumulative ventilation-rate distribution

Expressions (1) and (4) both relate the tracer inventory in a water mass of volume V to the mole-fraction history at the boundary of V , but the physical interpretations in terms of flux R in (1) and TTD in (4) appear distinct. However, (4) can be motivated directly from considerations of the flux of \mathcal{G} into the surface (Primeau and Holzer 2006). We show in the appendix that the following interpretation holds for steady-state transport:

$$\begin{aligned} \Phi(\tau) &\equiv \rho V \bar{\mathcal{G}}(\tau) \\ &= \begin{cases} \text{entering mass flux of water that will} \\ \text{reside at least time } \tau \text{ before exiting} \end{cases} \\ &= \begin{cases} \text{exiting mass flux of water that has} \\ \text{resided at least time } \tau \text{ since entering,} \end{cases} \end{aligned} \quad (5)$$

where V is the volume of the water mass being ventilated. Following the terminology of Primeau and Holzer (2006), we call $\Phi(\tau)$ the cumulative ventilation-rate distribution. For nonsteady-state transport, Φ and $\bar{\mathcal{G}}$ are closely related, but not proportional, as discussed in the appendix. We rewrite relationship (4) as

$$I(t) = \int_0^\infty C_0(t - \tau) \Phi(\tau) d\tau. \quad (6)$$

Note that because of the normalization $\int_0^\infty \mathcal{G}(\mathbf{r}, \tau) d\tau = 1$ [$\mathcal{G}(\mathbf{r}, \tau)$ is a PDF], one finds $\int_0^\infty \Phi(\tau) d\tau = \rho V$. Integrating the cumulative ventilation-rate distribution over all residence time thresholds simply results in the total water mass of the domain.

Primeau and Holzer (2006) have developed the cumulative ventilation-rate distribution and related diagnostics in greater generality, considering the case in which the surface entrance and exit regions of tracer do not necessarily coincide. They show that, if the entry and exit regions at least partially overlap and the flow has nonzero diffusivity, then the cumulative ventilation-rate distribution diverges as $\tau^{-1/2}$ in the limit of small τ . That is, the total ventilation rate $\Phi(0)$ —the gross flux of material that that resides any time at all in the domain—is infinite. Hall and Holzer (2003) came to the same conclusion in the context of stratosphere–troposphere exchange. A simple random-walk illustration of the small τ divergence independent of any particular geophysical domain may be found in Hall and Holzer (2003).

The cumulative ventilation-rate distribution, $\Phi(\tau)$, is a nonincreasing function because the flux of water that resides at least τ_2 must be less than or equal to the flux of material that resides at least $\tau_1 < \tau_2$, as the later includes the former. One can calculate the distribution, $\phi(\tau) \equiv -d\Phi(\tau)/d\tau$, such that $-\phi(\tau) \delta\tau$ is the flux of material that resides $(\tau, \tau + \delta\tau)$ before exiting. [In fact, it is $\phi(\tau)$ that Primeau and Holzer (2006) show is equivalent to the flux of \mathcal{G} into the surface.] However, unlike the TTD, $\phi(\tau)$ is not a PDF in the usual sense, at least in the case of coincident entry and exit regions, because it is not able to be normalized [$-\int_0^\infty \phi(\tau) d\tau = \Phi(0) = \infty$]. The distribution $\phi(\tau)$ partitions the flux into the domain according to the residence time of fluid

elements as they enter the domain and is completely dominated by the elements that reside infinitesimal time before exiting through the same surface.

3. General circulation model example

We turn now to an example from a general circulation model (GCM) to illustrate the cumulative ventilation-rate distribution, $\Phi(\tau)$. We will show that using $\Phi(\tau)$ reconciles disparate estimates of the GCM's ventilation rate made with different tracers. In the process we introduce and apply a statistical model of $\Phi(\tau)$ that is also applied in the subsequent analysis of observational data.

Haine et al. (2003, hereinafter HRJ) used two tracers to diagnose volume fluxes across the mixed layer base (which they call subduction rates) of various water masses in a North Atlantic GCM: a ventilation tracer, defined by a step-function concentration boundary condition at the surface, and CFC11. For each tracer a subduction rate, S (volume/time), was estimated by solving the budget equation:

$$\frac{dI}{dt} = S\rho C_{\text{enter}}(t) - S\rho C_{\text{exit}}(t), \quad (7)$$

where I is the tracer inventory (mass), ρ the water density, and $C_{\text{enter}}(t) = C_0(t)$ is the tracer mole fraction history (tracer mass/water volume) at the outcrop and $C_{\text{exit}}(t)$ is a tracer mole fraction chosen to characterize the returning water. (We use the symbol S for volume flux in this section to be consistent with HRJ.) Here S is assumed to be constant. For CFC11, HRJ take C_{exit} to be the average CFC11 mol fraction over the water mass, while for the ventilation tracer they assume that the mole fraction in the returning flux is negligible compared to that in the entering flux, at least over the period they analyze (months 6–18 following the onset of the ventilation-tracer's boundary condition). Solving the budget equation with these assumptions, HRJ obtain for CFC11

$$I_{\text{CFC}}(t) = S\rho \int_0^t dt' C(t') e^{S(t-t')/V}, \quad (8)$$

where V is the domain volume. Call this estimate $S = S_{\text{CFC}}$. [This expression for S is different from the simpler relationship (1) for R because of HRJ's inclusion of a nonzero returning CFC concentration.] For the ventilation tracer

$$I_{\text{VT}}(1 \text{ yr}) = \rho \int_{0.5\text{yr}}^{1.5\text{yr}} S dt = \rho S \times 1 \text{ yr}. \quad (9)$$

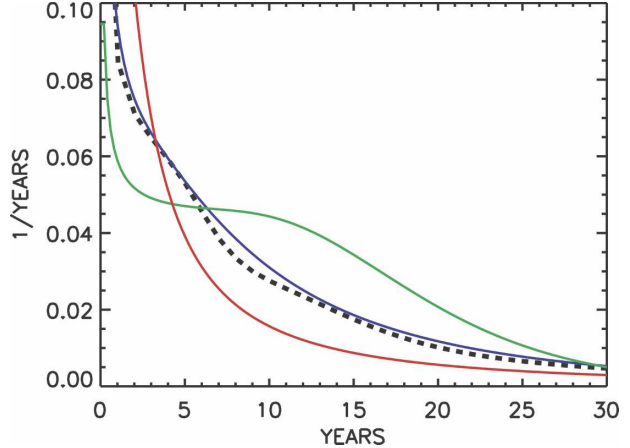


FIG. 1. GCM cumulative ventilation-rate distribution divided by the domain mass for STMW from the study of Haine and Hall (2002) (black, dashed). The colored solid lines are inverse Gaussian (IG) functional forms with mean residence time $\tau_M = 22$ yr, as simulated in the GCM, and Peclet number $P = 0.6$ (green), $P = 3$ (blue), and $P = 15$ (red). The case $P = 3$ fits the GCM distribution closely.

Call this estimate $S = S_{\text{VT}}$. STMW and SPMW are the two most rapidly ventilated masses in the HRJ model. HRJ find that $S_{\text{CFC}} \approx S_{\text{VT}}$ for STMW, while $S_{\text{CFC}} < S_{\text{VT}}$ for SPMW.

In light of the proper boundary propagation (4) it is clear that the estimates S_{CFC} and S_{VT} are related to the cumulative ventilation-rate distribution in different ways and will not, in general, be equal. To emphasize this we examine TTDs simulated in the same model, as reported by Haine and Hall (2002). [The precise model configuration of Haine and Hall (2002) differs slightly from that of HRJ, but the impact on this analysis is negligible.] Integrating the TTDs over the mass of STMW yields the GCM's cumulative ventilation-rate distribution for this water mass, which is shown in Fig. 1 divided by the total STMW mass. The GCM STMW $\Phi(\tau)$ is not well approximated by either a constant over some range, as would be necessary for (9) to be robust, or by a declining exponential, as would be necessary for (8) to be robust.

In contrast, the GCM's $\Phi(\tau)$ is well approximated by a two-parameter functional form related to the inverse Gaussian (IG) distribution (Fig. 1). The inverse Gaussian distribution is a useful statistical model of probability density functions with long tails (Seshadri 1999), such as the TTD at a point r with respect to some remote outcrop (a pointwise TTD). Because the cumulative ventilation-rate distribution is proportional to the volume-integrated TTD we employ a functional form obtained by integrating the IG TTD over a volume V :

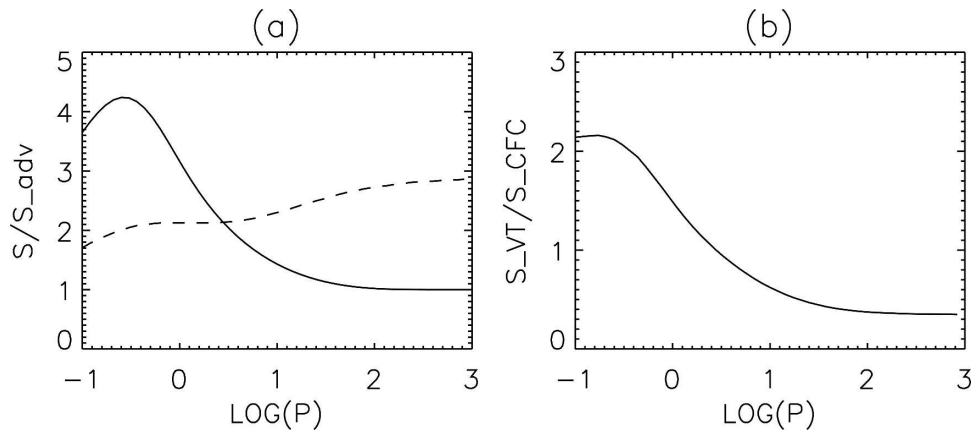


FIG. 2. (a) Volume flux estimates of HRJ, S_{VT} from expression (9) (solid) and S_{CFC} from expression (8) (dash) as functions of P . HRJ refer to these as subduction rates. Here, these are calculated using the inverse Gaussian form for the cumulative ventilation-rate distribution with $\tau_M = 22$ yr, the mean residence time for STMW in the HRJ GCM; S_{CFC} and S_{VT} are plotted divided by the value S_{VT} in the bulk advective (high P) limit.

$$\Phi(\tau) = \frac{V}{\sqrt{\pi P \tau_M \tau}} \left[e^{-P\tau/4\tau_M} - e^{-P(\tau_M - \tau)^2/4\tau_M\tau} \right] + \frac{1}{2\tau_M} \left\{ \operatorname{erf} \left[\sqrt{\frac{P\tau}{4\tau_M}} \right] + \operatorname{erf} \left[\sqrt{\frac{P}{4\tau_M\tau}} (\tau_M - \tau) \right] \right\}, \quad (10)$$

where τ_M is the mean residence time of water in volume V (τ_M is equal to 2 times the mean transit time), and the parameter P (Peclet number) is a measure of the departure of the transport from large-scale bulk advection. Several examples of IG $\Phi(\tau)$ are shown in Fig. 1, along with the GCM's $\Phi(\tau)$. In the bulk-advective limit $P = \infty$, and each point in V is reached by a unique pathway with a single transit time. All such transit times are equally represented up to some threshold, which is the “oldest” water in V , associated with the most distant point from the outcrop. Hence, in the bulk-advective limit $\Phi(\tau)$ is a step function. More generally (P finite), while there may be a dominant advective pathway from the outcrop to a point r in V with a narrow range of short transit times, eddy mixing also gives rise to a multiplicity of longer convoluted pathways with a wide range of transit times. The step function in $\Phi(\tau)$ is smoothed, or disappears entirely (depending on P), and there is more representation at both short and long transit times.

The IG distribution has been shown to mimic well directly integrated TTDs in numerical models (Khatiwala et al. 2001; Haine and Hall 2002; Primeau 2005; Peacock and Maltrud 2006). This is clearly true for STMW in the HRJ model, as seen in Fig. 1. A close fit to the GCM's Φ is provided by setting $\tau_M = 22$ yr, the mean residence time for STMW in the GCM, as determined by Haine and Hall (2002), and $P = 3$, determined by minimizing the IG – GCM difference.

To understand better the relationship between S_{CFC} and S_{VT} we use the IG model to generate estimates S_{CFC} and S_{VT} for a range of P . Here I_{CFC} is computed using (4), and S_{CFC} is chosen to fit (8) best. The value S_{VT} is simply $\Phi(\tau)$ averaged from $\tau = 0.5$ to 1.5 yr. Figure 2a shows the two estimates as a function of P for STMW, and Fig. 2b shows their ratio. For the best-fit value $P \approx 3$, we find that $S_{CFC} \approx S_{VT}$, in agreement with HRJ. However, the agreement is not robust; at smaller P , $S_{CFC} < S_{VT}$, while at larger P , $S_{CFC} > S_{VT}$. For SPMW, HRJ found $S_{VT}/S_{CFC} \approx 1.8$. The corresponding domain-averaged TTD was found by Haine and Hall (2002) to have a mean transit time of 82 yr, corresponding to $\tau_m = 164$ yr. Figures 3a,b are similar to Figs. 2a,b, respectively, but now for the GCM's SPMW. The range $1 < P < 10$ yields $1.8 > S_{VT}/S_{CFC} > 1.6$, in agreement with HRJ.

We conclude that the disparate estimates of ventilation rates made by HRJ using two different tracers can be reconciled by considering the cumulative ventilation-rate distribution. The analysis corroborates the idea that no single flux can fully characterize the ventilation of a water mass.

4. Cumulative ventilation-rate distributions estimated from CFC observations

We now estimate cumulative ventilation-rate distributions from North Atlantic CFC11 observations for

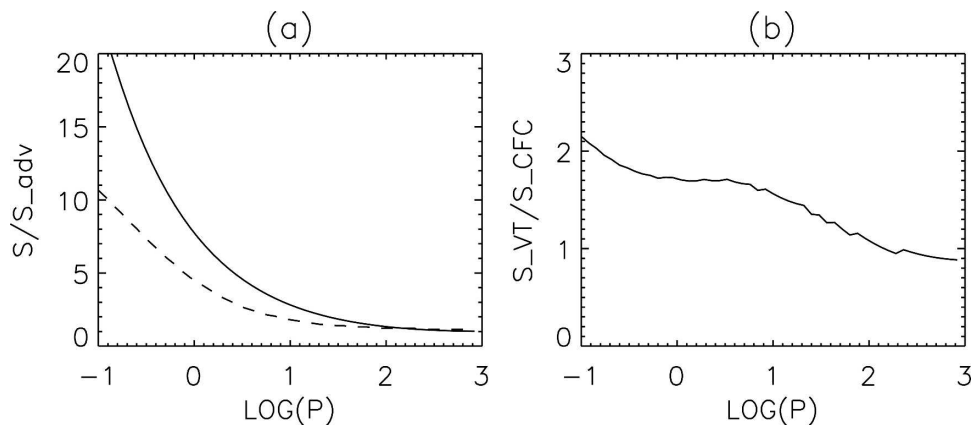


FIG. 3. As in Fig. 2 but with $\tau_M = 164$ yr, the mean residence time for SPMW in the HRJ GCM.

STMW and LSW. We first define the domains and their formation regions, then estimate CFC inventories and formation-region time histories, and finally constrain the cumulative ventilation-rate distribution using the IG functional form. The data are WOCE CFC11 measurements from 1996–98 that have been mapped and gridded onto 18 neutral density surfaces (see www.ideo.columbia.edu/~lebel/inventory_maps.html for details, and the acknowledgment section for the principal investigators responsible for data collection). Only the subset of these data comprising STMW and LSW are used here. The CFC11 distribution on these isopycnal slabs is shown in Fig. 4, and the volumes, CFC11 inventories, and mean mole fractions are listed in Table 1.

a. Domain definitions

The closed domains are bounded by neutral density surfaces, the sea surface, and the equator. Each domain

is divided into two subdomains: the mixed layer and the interior. Water in the mixed layer is in rapid contact with the sea surface via vertical mixing and deep convection. We estimate the time history of the mean CFC11 mol fraction in the mixed layer and take this as the time-dependent CFC11 boundary condition, assumed to be spatially uniform on the mixed layer base. This boundary condition is transported from the formation region into the interior, and the cumulative ventilation-rate distribution diagnoses the flux into the interior. The circulation is assumed to be steady.

The bounding neutral density surfaces for STMW are $\gamma_n = 26.025$ and 26.645 . STMW formation is known to occur in the western mid Atlantic at the southern flank of the Gulf Stream. The precise region of formation is uncertain, but a characteristic feature of the formation of all mode water is vertical homogeneity over a thick region (large separation between the density surfaces).

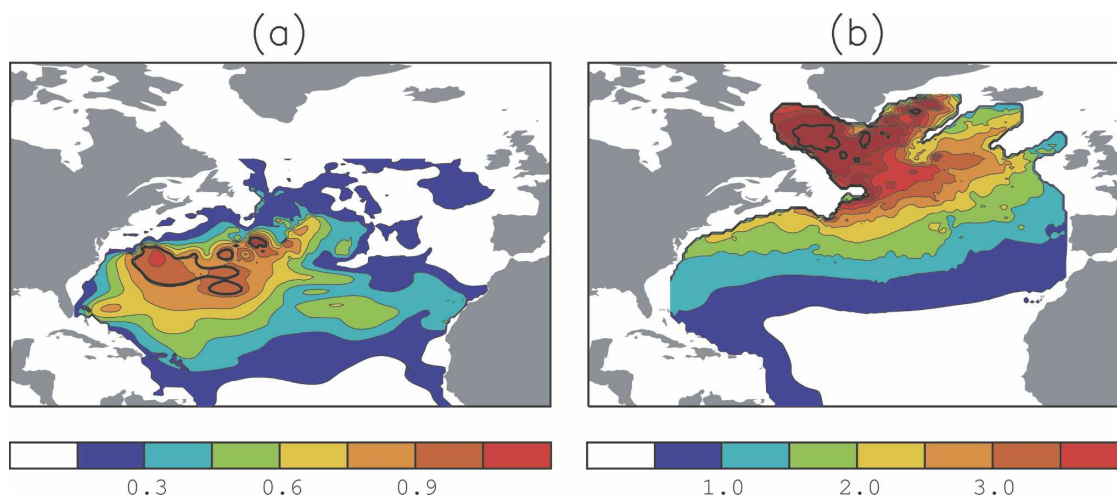


FIG. 4. CFC11 mass per area for (a) STMW and (b) LSW ($\mu\text{mol m}^{-2}$). Also shown (heavy contour) are the assumed formation regions, defined as areas whose water-mass thickness is greater than 400 m (STMW) and 1600 m (LSW).

TABLE 1. Water-mass density, volume, CFC11 mass, mean CFC11 concentration, and ratio of mean CFC11 concentration to outcrop concentration (fraction). The defined formation regions are excluded from the total volumes and inventories.

Name	Neutral density	Volume	Mass	Concentration	Fraction
STMW	26.025–26.645	$3.1 \times 10^{15} \text{ m}^3$	$6.4 \times 10^6 \text{ mol}$	2.1 pmol l^{-1}	0.92
LSW	27.897–27.985	$2.0 \times 10^{16} \text{ m}^3$	$2.0 \times 10^7 \text{ mol}$	1.0 pmol l^{-1}	0.27

We use thickness as a criterion defining the formation region: all STMW with thickness greater than 400 m is taken to be part of the formation region (Fig. 4). There is some arbitrariness in this threshold, and different thresholds result in slightly different inferred $\Phi(\tau)$.

The bounding density surfaces for LSW are $\gamma_n = 27.897$ and 27.985 . There is less arbitrariness in specifying the LSW formation region because it is bounded geographically by the Labrador Sea. For consistency with the STMW analysis, however, we use a thickness criterion here too, in this case 1600 m. Figure 4 shows this region to be mostly in the Labrador Sea, although there are small patches south and east of southern Greenland.

b. Constraining $\Phi(\tau)$

Water in the interior of the domain is supplied by the cumulative ventilation-rate distribution acting on water in the formation region, and it is the CFC11 inventory of the interior that is used to estimate the cumulative ventilation-rate distribution. We compute the interior CFC11 inventory, I_{CFC} , by subtracting the inventory of the formation region from the inventory of the entire region. To estimate the CFC11 mol fraction history in the formation region, $C_0(t)$, we scale the Northern Hemisphere atmospheric time history of Walker et al. (2000) by a single number to match the mean CFC11 mol fraction in the formation region in 1997, a procedure that implicitly accommodates subsaturation, albeit imperfectly. [The resulting mole fraction is 67% of the saturated equilibrium value in 1997, consistent with estimates of Smethie and Fine (2001).] Here I_{CFC} , $\Phi(\tau)$, and $C_0(t)$ are related via relationship (6), and constraining $\Phi(\tau)$ amounts to inverting (6). We perform this inversion parametrically; that is, we assume that $\Phi(\tau)$ has the two-parameter IG form (9) and find values of the parameters, τ_M and P , that satisfy relationship (6). Because a single inventory datum cannot simultaneously constrain two parameters, we obtain a family of Φ consistent with the data, from strong mixing (low P , high τ_M) to bulk advection (high P , low τ_M).

This procedure to constrain $\Phi(\tau)$ with CFCs is identical to the analysis of Hall et al. (2004), who constrained $\bar{g}(\tau)$ (the domain-averaged TTD) for Indian Ocean water masses. Hall et al. did not invoke the flux

interpretation, but instead immediately applied $\bar{g}(\tau)$ to estimate anthropogenic carbon inventories. Our estimates here of $\Phi(\tau)$ in the North Atlantic could also be applied to anthropogenic carbon, given knowledge of its history in surface waters. Carbon is not the focus in this study, but we have pursued the application in a related study of LSW (Terenzi et al. 2007).

Figures 5a and 5b show samples of $\rho^{-1}\Phi(\tau)$ for STMW and LSW, where ρ is the water density. (For consistency with previous estimates we divide by ρ to obtain units of volume flux, expressed in Sverdrups.) In the bulk-advective limit (large P) the flux supplying STMW is about 6 Sv for all residence-time thresholds up to 16 yr. No water resides in STMW longer than 16 yr, in this limit. In the strong-mixing limit (low P) the flux declines monotonically with residence time. At residence-time thresholds less than about 3 yr the strong-mixing flux is greater than the bulk-advective flux. Between 3 and 16 yr it is less than the advective flux. With mixing present the flux of water mass that resides more than 16 yr is nonzero. The relative relationships among the cumulative ventilation-rate distributions for LSW are similar, but the bulk-advective flux is larger (8.5 Sv) and supplies water to greater residence times (76 yr).

A wide range of ventilation scenarios is consistent with the CFC11 inventory. Figure 6 shows the CFC11-constrained $\rho^{-1}\Phi$ as a function of P for four different residence-time thresholds: $\tau = 1, 10, 60,$ and 100 yr. The flux supplying STMW that will reside at least 1 yr ranges from 6 to 20 Sv, while the flux that will reside at least 10 yr ranges from 0.5 to 6 Sv. For STMW there is negligible flux of water that resides more than about 30 yr, so the curves for $\tau = 60$ and 100 yr are zero. The fluxes supplying LSW that reside 1, 10, 60, and 100 yr are 9–20, 6–9, 2–9, and 0–2 Sv, respectively.

Additional information can narrow these wide ranges of ventilation rates. Waugh et al. (2004) used CFCs and bomb tritium in combination to estimate two-parameter pointwise IG TTDs at various locations in the subpolar North Atlantic. Although precise parameter pairs could not always be obtained, Waugh et al. were consistently able to put an upper bound of $P \approx 3$. These P bounds indicate that the bulk-advective (high P) regime of $\Phi(\tau)$ is not realistic. Other independent

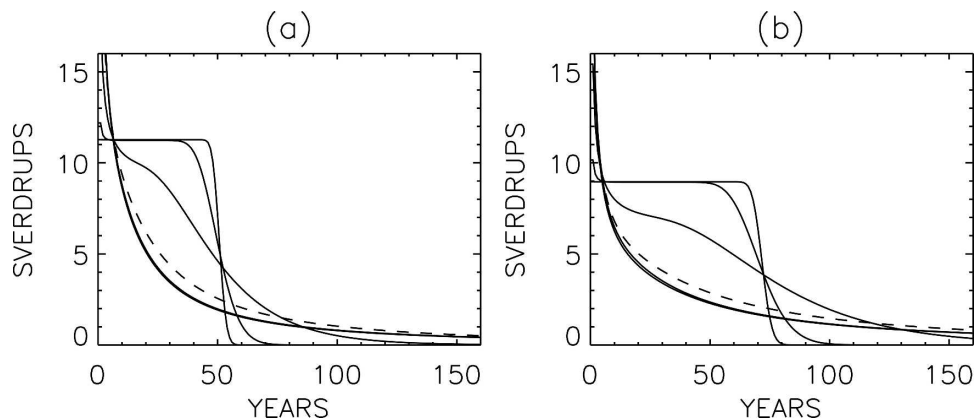


FIG. 5. Cumulative ventilation-rate distributions, $\Phi(\tau)$, consistent with North Atlantic CFC11 observations in (a) STMW and (b) LSW. For each water mass four Φ are shown with mean residence time t_M and Peclet number P consistent with the observations. Listed from most steeply declining to most steeply Φ the parameter pairs (t_M, P) are for STMW: (24 yr, 0.1), (12 yr, 3), (14 yr, 10), and (16 yr, 1000); and for LSW: (3340 yr, 0.1), (176 yr, 3), (102 yr, 10), and (72 yr, 1000). For reference, the Φ with $P = 3$ are plotted dashed, while the Φ with $P \leq 3$ are plotted black and the distributions with $P > 3$ are plotted gray.

estimates of P give similar magnitudes. Jenkins (1988) inferred a value $P = 1$ –2 from tritium measurements in the North Atlantic, while O'Dwyer et al. (2000) infer a mean $P \approx 4$ from North Atlantic float data. If we assume a more narrow range $P = 0$ –3 in our analysis, then we obtain a correspondingly smaller range of $\Phi(\tau)$. These tighter bounds on STMW $\rho^{-1}\Phi(\tau)$ at residence times thresholds 1 and 10 yr are 13–20 and 0.5–2.5 Sv, respectively. The tighter bounds on LSW $\rho^{-1}\Phi(\tau)$ at residence times thresholds 1, 10, 60, and 100 yr are 17–20, 6–7, 2–3, and 1–2 Sv, respectively.

Additional uncertainties apply that we have not included here. CFC11 mol fractions are measured to high accuracy. However, the inventories are formed from

sparse data and are, therefore, subject to a random sampling error of at least $\pm 10\%$. [Rhein et al. (2002) estimate a 10% uncertainty for the Labrador Sea region, but our region encompasses the subtropics, which are sampled less densely.] These errors apply separately to the interior and formation regions of the domain, and so the combined effect on the inference of the ventilation rate distribution is larger. Important is that we have assumed transport to be in steady state. At best, our inferred ventilation-rate distribution approximates a time average of the true distribution. However, the nonlinear CFC11 surface-water history coupled with significant decadal variability could bias our estimate of $\Phi(\tau)$. In general our methodology applies

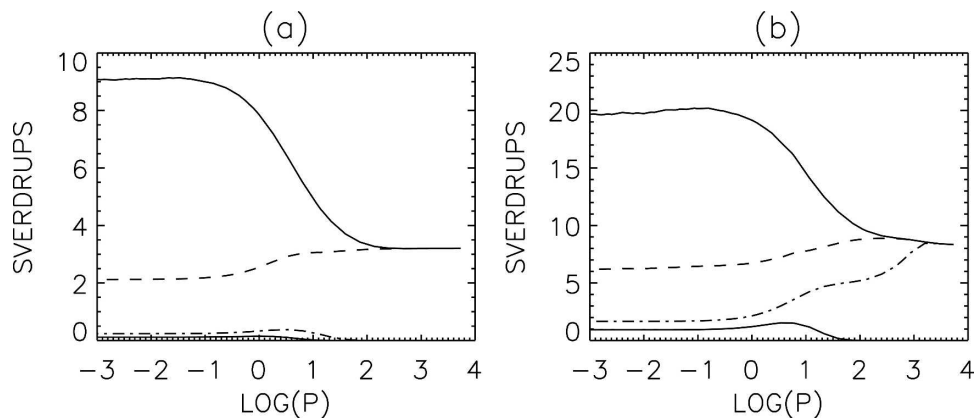


FIG. 6. The CFC11-constrained cumulative ventilation-rate distributions for (a) STMW and (b) LSW, evaluated as a function of Peclet number at four different residence times: $\Phi(1\text{yr})$ (top solid), $\Phi(10\text{yr})$ (dash), $\Phi(60\text{ yr})$ (dot-dash), and $\Phi(100\text{ yr})$ (bottom solid). For STMW the flux that resides more than about 30 yr for any P is negligible (Fig. 5a), so the curves $\Phi(60\text{ yr})$ and $\Phi(100\text{ yr})$ are not visible.

equally well to the time-varying case. In practice a functional form for $\Phi(\tau)$ would have to be adopted that has additional degrees of freedom, and these would require additional information as constraints. Even for the steady-state case error is possible if the ventilation rate distribution is not well fit by a volume-averaged inverse Gaussian form, although, as we have noted the inverse Gaussian fits well $\Phi(\tau)$ simulated directly in GCMs.

5. Analysis of previous tracer methods

As discussed in the introduction, several studies have applied variants of relationship (1) to CFC inventories derived from observations to estimate water-mass formation rates (Smethie and Fine 2001; Rhein et al. 2002; Kieke et al. 2006). For various components of North Atlantic Deep Water, Smethie and Fine (2001) express the CFC11 inventory as a sum over the yearly history of CFC11 $I = \sum R\rho C_0\Delta t$, where C_0 is the CFC11 mol fraction each year in the source region, R is their formation-rate estimate, and $\Delta t = 1$ yr. In one case R is assumed constant, while in another R is allowed to vary with calendar date. Similarly, Rhein et al. (2002) write for LSW $R = I/\int_{1930}^{1997} \rho s C_{\text{eq}}(t) dt$, where $C_{\text{eq}}(t)$ is the mole fraction in the Labrador Sea that would be in equilibrium with the atmosphere, and s is the degree of saturation ($C_0 = sC_{\text{eq}}$). Kieke et al. (2006) look at the evolution over two years of the CFC11 inventory of the upper density component of LSW, obtaining a formation rate estimate $R = [I(t_2) - I(t_1)]/\int_{t_1}^{t_2} \rho s C_{\text{eq}}(t) dt$.

Although the definitions of the formations regions and interior domains differ, the relationships used to calculate the formation rates are equivalent to expression (1), which does not provide for any dependence on residence time. Consider the case of steady-state transport. The more general expression (6) reduces to the expressions used in the papers cited above only if Φ is approximately independent of residence time over the range from 0 to ~ 50 yr (the history of the CFCs). The expression used by Kieke et al. (2006) can be derived from (6) only if Φ is independent of residence time over the range zero to $t_2 - t_1 = 2$ yr. However, judging from the GCM example (Fig. 1) and from observationally based examples in a realistic P regime (Fig. 5), $\Phi(\tau)$ is highly sensitive to τ over both these intervals. Assuming τ -independent ventilation appears to be a poor approximation.

One spurious consequence of neglecting the τ dependence of Φ is that the resulting formation-rate estimates are time-dependent, even when the underlying transport is constant. To illustrate this point we have estimated

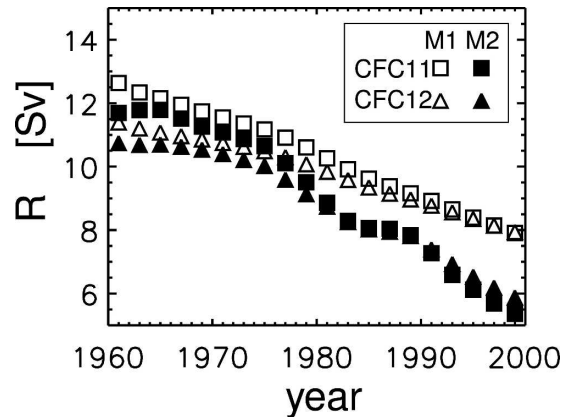


FIG. 7. Formation-rate $R(t)$ estimated using two published methods, M1 and M2, and two tracers, CFC11 and CFC12. The methods are M1: $R_1 = I(t)/\int_{1930}^t \rho C_0(t') dt'$, as in Rhein et al. (2002); and M2: $R_2 = [I(t) - I(t - \Delta t)]/\int_{t-\Delta t}^t \rho C_0(t') dt'$ with $\Delta t = 2$ yr, as in Kieke et al. (2006); $I(t)$ is the CFC inventory in LSW; $C_0(t)$ is the CFC mole fraction in the formation region, as defined in the text; and ρ is the water density. In both cases $I(t)$ is computed via expression (6) from $C_0(t)$ and the steady-state cumulative ventilation rate distribution, $\Phi(\tau)$. The IG form for $\Phi(\tau)$ is used, with parameter values $P = 3$ and $\tau_M = 176$ yr (Fig. 5), within the realistic regime. Despite the steady-state ventilation, the formation rates estimates decline in time. This is purely an artifact of the erroneous neglect of the τ dependence of Φ in the expressions for R_1 and R_2 .

the time-dependent CFC11 inventory, $I(t)$, in LSW using the formation-region mole fraction history, $C_0(t)$, of section 4, $\Phi(\tau)$ in Fig. 5b with $P = 3$; and relationship (6). The formation rate is then estimated at a range of dates from $I(t)$ and $C_0(t)$ according to two methods: 1) $R_1 = I(t)/\int_{1930}^t \rho C_0(t') dt'$, as in Rhein et al. (2002) for steady transport; and 2) $R_2 = [I(t) - I(t - \Delta t)]/\int_{t-\Delta t}^t \rho C_0(t') dt'$, with $\Delta t = 2$ yr, as in Kieke et al. (2006). Figure 7 shows the results. Also shown are the same rates inferred from CFC12. The estimated rate depends on the method employed and (for earlier years) on the tracer. In addition, despite the fact that the transport is steady, all the rate estimates decline in time. The $R_1 - R_2$ difference, the tracer dependence, and the time-dependence are all artifacts of the erroneous assumption that ventilation is independent of residence time, which is equivalent to the assumption that transport is purely bulk advective. [Tracer ages can exhibit spurious time dependence for the same reason (Waugh et al. 2003).] Any conclusion about evolving circulation from such an analysis should be regarded with caution.

Böning et al. (2003) have estimated LSW formation rates using a volumetric method (volume change of the density class over a year) in a high-resolution North Atlantic GCM. They obtain values varying between

0–11 Sv from 1970 to 1995. Böning et al. also perform a CFC11-based analysis, using method 1 above of Rhein et al. (2002), and obtain the range 3.4–4.4 Sv. While their CFC11 range encompasses their time-averaged volumetric estimate for the years 1970–95, it is not clear that this is robust. Given such large fluctuations in the volumetric rate, a different averaging period would result in a substantially different mean, presumably degrading the agreement with the CFC11 estimate.

We note that Sarmiento (1983) used bomb tritium data to estimate STMW volume exchange between surface waters and the thermocline. His analysis is similar to the Haine et al. (2003) CFC analysis (section 3) in that waters returning to the surface layer were assumed to have a tritium mole fraction equal to the domain-averaged mole fraction. The difference between the Sarmiento (1983) STMW flux estimate and the estimate of Haine et al. (2003) can be understood at least in part by considering the cumulative ventilation rate distribution. The assumption of a domain-averaged mole fraction for the returning waters is equivalent to the assumption of an exponential form for $\Phi(\tau)$, which misses key features of $\Phi(\tau)$ (section 3). As a consequence the flux estimates are tracer dependent.

6. Conclusions

The advective–diffusive transport of material across the mixed layer base cannot be characterized by a single flux, even for steady circulation. We have introduced a cumulative ventilation-rate distribution, $\Phi(\tau)$, which is the mass flux into an ocean domain that will reside at least time τ before exiting or, equivalently (in steady state), the mass flux out of the domain of water that has resided at least τ . We show that $\Phi(\tau)$ is equal to the transit-time distribution mass-integrated over the domain being ventilated. Only for pure bulk advection is the total one-way flux $\Phi(0)$ finite and representative of large-scale transport. In the presence of any diffusive mixing $\Phi(0) = \infty$. $\Phi(\tau)$ at small τ is dominated by rapid back-and-forth motion that penetrates only short distances beyond the mixed layer base, and, thus, the total one-way flux is not a useful diagnostic of large-scale transport. As a function of τ , however, Φ is an integrable, monotonically declining function that diagnoses the ventilation of a water mass over a continuous range of residence times.

We have shown that the common practice of neglecting any residence-time dependence of ventilation when relating the inventory and the mixed layer history of transient tracers can lead to misinterpretation, in the presence of mixing. The ventilation-rate estimate obtained in this way is dependent on the particular tracer

and varies in time with the tracer's evolution, even for steady transport.

By contrast, the cumulative ventilation-rate distribution is a flux diagnostic independent of any particular tracer. While in general its relationship to the fluid flow's velocity and diffusivity field is not simple, $\Phi(\tau)$ nonetheless summarizes the transport in a way that is immediately applicable to tracers. We have used the cumulative ventilation-rate distribution to reconcile disparate estimates of ventilation rates from two different tracers in a GCM study, thereby corroborating its utility. Using a two-parameter statistical model we have bounded $\Phi(\tau)$ for Subtropical Mode Water and Labrador Sea Water using North Atlantic CFC11 observations.

The necessity to characterizing the flux into a water mass by a distribution rather than a single number is a key point of our work. However, for convenient comparisons among water masses it may be desirable to use a single values of flux. For example, one could choose as a convention the flux of water that resides at least $\tau = 10$ yr, as long as it is acknowledged that this flux does not fully characterize the ventilation.

Our analysis of STMW and LSW is limited by the assumption of steady-state transport. It is well known that the formation and ventilation of North Atlantic waters undergoes interannual variability. The key point, however, that no single ventilation rate value can summarize the flux of water across the mixed layer base, is equally valid in the presence of time-varying transport. Tracer concentrations can still be written as convolutions with a domain-averaged TTD, but the TTD has explicit time variation (e.g., Holzer and Hall 2000). In practice, one could, for example, generalize the functional form used for Φ to include a periodic cycle, thereby increasing from two to five the number of free parameters (τ_A , P , and the amplitude, frequency, and phase of the periodicity). One could attempt to make use of other tracers or circulation information to remove some of these degrees of freedom. This approach would be a generalization to include mixing of the approach of Smethie and Fine (2001), who added decadal periodicity to a ventilation analysis using CFCs.

Acknowledgments. This work has been supported by National Science Foundation Grants OCE-0326860 and OCE-9811034 and by the National Aeronautics and Space Administration. We are grateful for the efforts of the many researchers involved in making CFC measurements. The principal investigators for the CFC11 measurements used in this analysis were C. Andrie, W. Roether, L. Memery, W. Smethie, M. Rhien, P. Jones, R. Weiss, D. Smythe-Wright, and J. Bullister.

APPENDIX

Derivation of the Ventilation-Rate Distribution

We derive here the cumulative ventilation-rate distribution in terms of the boundary propagator, or transit-time distribution. Consider an idealized tracer at time t responding to a Heaviside concentration boundary condition on a surface region Ω and a no-flux condition on all other boundaries; that is, on Ω the concentration is zero at all times before t_0 and unity thereafter. We restrict attention to a domain of volume V having uniform and constant water density ρ . While the arguments below can be adapted to any closed domain with a boundary region Ω on which tracer concentration conditions are applied, we generally think of the domain as being an isopycnal interior ocean volume whose intersection with the mixed layer constitutes the surface area Ω . Fluid elements in V that have made contact with Ω within the elapsed time $t - t_0$ carry a tracer concentration of unity, while those that have not carry a tracer concentration of zero. The tracer inventory, $I_{VT}(t, t_0)$, evolves from zero at $t = t_0$ to the total water mass, ρV , at $t = \infty$; that is, eventually all the fluid elements make contact with Ω and receive a tracer label. For any time t

$$I_{VT}(t, t_0) = \begin{cases} \text{water mass in } V \text{ at } t \text{ that} \\ \text{has been labeled by tracer,} \\ \\ \text{water mass in } V \text{ that has made} \\ \text{contact with } \Omega \text{ within } t - t_0. \end{cases} \quad (\text{A1})$$

It follows that $\rho V - I_{VT}(t, t_0)$ is the water mass that has not made Ω contact within $t - t_0$. This water has resided in V longer than $t - t_0$ since last Ω contact. The rate of change $(d/dt)[\rho V - I_{VT}(t, t_0)] = -dI_{VT}/dt$ is the rate (mass/time) at which the water mass that is unlabeled by tracer declines. It is the rate at which unlabeled water makes contact with Ω . In other words, dI_{VT}/dt is the mass flux into Ω of water that has resided in V longer than $t - t_0$. [One might at first balk at the flux interpretation and simply ascribe the reduction of $\rho V - I_{VT}(t, t_0)$ to the progressively deeper penetration of the tracer signal. However, if the domain has finite and constant water mass, then for every newly labeled fluid element just entering the domain following Ω contact there must be an unlabeled fluid element just exiting the domain by Ω contact.] The fate of the fluid elements following Ω contact depends on the location of Ω and the circulation outside V . If Ω is on the mixed layer base, then fluid elements can pass through Ω to enter the mixed layer. If Ω is on the ocean surface, there is no passage through Ω . However, fluid elements undergo-

ing random walks due to diffusive processes can impact Ω , receive a tracer label, and reflect back into the domain.

Following the notation of Primeau and Holzer (2006) we denote this mass flux of water, dI_{VT}/dt , as $\Phi_{\uparrow}(t, \tau)$, where $\tau = t - t_0$. Now, I_{VT} can be related to $\bar{G}(t, t')$ by the defining properties of the boundary propagator and the Heaviside condition:

$$I_{VT}(t, t_0) = \rho V \int_{t_0}^t dt' \bar{G}(t, t') = \rho V \int_0^{t-t_0} d\xi \bar{G}(t, t - \xi).$$

Thus, taking the t derivative, we have

$$\Phi_{\uparrow}(t, \tau) = \rho V \bar{G}(t, t_0) + \rho V \int_0^{\tau} d\xi \frac{\partial}{\partial t} \bar{G}(t, t - \xi) \quad (\text{A2})$$

is the flux of water mass into Ω (exiting V) that has resided at least $\tau = t - t_0$ in V .

To obtain the interpretation in terms of the flux entering V , consider the difference between a tracer response to a Heaviside onset at t_0 and an onset at $t_0 + \delta t_0$. The quantity $M(t, t_0) = \rho V - I_{VT}(t, t_0)$ is the water mass that has not made Ω contact within $t - t_0$, and $M(t, t_0 + \delta t_0) = \rho V - I_{VT}(t, t_0 + \delta t_0)$ is the water mass that has not made Ω contact within $t - (t_0 + \delta t_0)$. The difference $M(t, t_0 + \delta t_0) - M(t, t_0) > 0$ is the water mass that entered the domain in the interval $(t_0, t_0 + \delta t_0)$ and is still in the domain at time t . The rate at which this newly labeled water mass increases, $dM/dt_0 = -dI_{VT}/dt_0$, is the mass flux into V from Ω of water that will reside at least $\tau = t - t_0$. By the definitions of the Heaviside and the boundary propagator $-dI_{VT}/dt_0 = \rho V \bar{G}(t, t_0)$. We have, then, that

$$\Phi_{\downarrow}(t - \tau, \tau) = \rho V \bar{G}(t, t_0) \quad (\text{A3})$$

is the mass flux into V from Ω at time $t - \tau = t_0$ of water that will reside at least τ before exiting. [See Primeau and Holzer (2006) for a different derivation.]

If the circulation is in steady state, then \bar{G} depends on t and t_0 only through their difference, $t - t_0 \equiv \tau$. The second term on the right-hand side of (A2) vanishes so that $\Phi_{\uparrow}(t, \tau) = \Phi_{\downarrow}(t - \tau, \tau)$, which we write as

$$\begin{aligned} \Phi(\tau) &\equiv \rho V \bar{G}(\tau) \\ &= \begin{cases} \text{entering mass flux of water that will} \\ \text{reside at least time } \tau \text{ before exiting} \end{cases} \\ &= \begin{cases} \text{exiting mass flux of water that has} \\ \text{resided at least time } \tau \text{ since entering,} \end{cases} \end{aligned} \quad (\text{A4})$$

Following the terminology of Primeau and Holzer (2006), we call $\Phi(\tau)$ the cumulative ventilation-rate distribution.

For time-varying transport the second term on the right of (A2) is nonzero, and we have

$$\Phi_{\uparrow}(t, \tau) - \Phi_{\downarrow}(t - \tau, \tau) = \rho V \int_0^{\tau} d\xi \frac{\partial}{\partial t} \bar{G}(t, t - \xi). \quad (\text{A5})$$

This difference term accounts for the fact that the explicit time variation of the transport can enhance or hinder the rate at which water makes contact with Ω . For example, if the circulation is slowing—the water is becoming “older”—the fraction of \bar{G} greater than τ is increasing, while the fraction less than τ is decreasing, so that the right-hand side of (A5) is negative. Consistent with this aging is a reduced flux out of V of old water (residence time greater than τ) relative to the flux at past times into V that will achieve at least an age of τ .

REFERENCES

- Beining, P., and W. Roether, 1996: Temporal evolution of CFC-11 and CFC-12 concentrations in the ocean interior. *J. Geophys. Res.*, **101**, 16 455–16 464.
- Böning, C. W., M. Rhein, J. Dengg, and C. Dorow, 2003: Modeling CFC inventories and formation rates of Labrador Sea Water. *Geophys. Res. Lett.*, **30**, 1050, doi:10.1029/2002GL014855.
- Deleersnijder, E., J.-M. Campin, and E. J. M. Delhez, 2001: The concept of age in marine modelling, 1, Theory and preliminary model results. *J. Mar. Syst.*, **28**, 229–267.
- Haine, T. W. N., and T. M. Hall, 2002: A generalized transport theory: Water–mass composition and age. *J. Phys. Oceanogr.*, **32**, 1932–1946.
- , K. J. Richards, and Y. Jia, 2003: Chlorofluorocarbon constraints on North Atlantic Ocean ventilation. *J. Phys. Oceanogr.*, **33**, 1798–1814.
- Hall, T. M., and M. Holzer, 2003: Advective–diffusive mass flux and implications for stratosphere–troposphere exchange. *Geophys. Res. Lett.*, **30**, 1222, doi:10.1029/2002GL016419.
- , D. W. Waugh, T. W. N. Haine, P. E. Robbins, and S. Khatiwala, 2004: Estimates of anthropogenic carbon in the Indian Ocean with allowance for mixing and time-varying air–sea disequilibrium. *Global Biogeochem. Cycles*, **18**, GB1031, doi:10.1029/2003GB002120.
- Hazeleger, W., and S. S. Drijfhout, 2000: Eddy subduction on a model of the subtropical gyre. *J. Phys. Oceanogr.*, **30**, 677–695.
- Holzer, M., and T. M. Hall, 2000: Transit-time and tracer-age distributions in geophysical flows. *J. Atmos. Sci.*, **57**, 3539–3558.
- Jenkins, W. J., 1988: The use of anthropogenic tritium and helium-3 to study subtropical ventilation and circulation. *Philos. Trans. Roy. Soc. London*, **325A**, 43–61.
- Khatiwala, S., M. Visbeck, and P. Schlosser, 2001: Age tracers in an ocean GCM. *Deep-Sea Res. I*, **48**, 1423–1441.
- Kieke, D., M. Rhein, L. Stramma, W. Smethie, D. A. LeBel, and W. Zenk, 2006: Changes in the CFC inventories and formation rates of upper Labrador Sea Water. *J. Phys. Oceanogr.*, **36**, 64–86.
- Marsh, R., 2000: Recent variability of the North Atlantic thermohaline circulation inferred from surface heat and freshwater fluxes. *J. Climate*, **13**, 3239–3260.
- Marshall, J. C., A. J. G. Nurser, and R. G. Williams, 1993: Inferring the subduction rate and period over the North Atlantic. *J. Phys. Oceanogr.*, **23**, 1315–1329.
- , D. Jamous, and J. Nilsson, 1998: Reconciling “thermodynamic” and “dynamic” methods of computation of water-mass transformation rates. *Deep-Sea Res. I*, **46**, 545–572.
- O’Dwyer, J., R. G. Williams, J. H. LaCasce, and K. G. Speer, 2000: Does the potential vorticity distribution constrain the spreading of floats in the North Atlantic. *J. Phys. Oceanogr.*, **30**, 721–732.
- Orsi, A. H., G. C. Johnson, and J. L. Bullister, 1999: Circulation, mixing, and production of Antarctic Bottom Water. *Prog. Oceanogr.*, **43**, 55–109.
- Peacock, S., and M. Maltrud, 2006: Transit-time distributions in a global ocean model. *J. Phys. Oceanogr.*, **36**, 474–495.
- Primeau, F. W., 2005: Characterizing transport between the surface mixed layer and the ocean interior with a forward and adjoint global ocean transport model. *J. Phys. Oceanogr.*, **35**, 545–564.
- , and M. Holzer, 2006: The ocean’s memory of the atmosphere: Residence-time distributions and water-mass ventilation. *J. Phys. Oceanogr.*, **36**, 1439–1456.
- Rhein, M., and Coauthors, 2002: Labrador Sea Water: Pathways, CFC inventory, and formation rates. *J. Phys. Oceanogr.*, **32**, 648–665.
- Robbins, P. E., J. F. Price, W. B. Owens, and W. J. Jenkins, 2000: The importance of lateral diffusion for the ventilation of the lower thermocline in the subtropical North Atlantic. *J. Phys. Oceanogr.*, **30**, 67–89.
- Sarmiento, J. L., 1983: A tritium box model of the North Atlantic thermocline. *J. Phys. Oceanogr.*, **13**, 1269–1274.
- Seshadri, V., 1999: The inverse Gaussian distribution. *Lecture Notes in Statistics*, Springer-Verlag, 1–347.
- Smethie, W. M., and R. A. Fine, 2001: Rates of North Atlantic deep water formation calculated from chlorofluorocarbon inventories. *Deep-Sea Res. I*, **48**, 189–215.
- Speer, K., and E. Tziperman, 1992: Rates of water mass formation in the North Atlantic Ocean. *J. Phys. Oceanogr.*, **22**, 94–104.
- Terenzi, F., T. M. Hall, S. Khatiwala, and D. A. LeBel, 2007: Uptake of natural and anthropogenic carbon by the Labrador Sea. *Geophys. Res. Lett.*, **34**, L06608, doi:10.1029/2006GL028543.
- Walín, G., 1982: On the relation between sea-surface heat flow and thermal circulation in the ocean. *Tellus*, **34**, 187–195.
- Walker, S. J., R. F. Weiss, and P. K. Salameh, 2000: Reconstructed histories of the annual mean atmospheric mole fraction for the halocarbons CFC11, CFC12, and carbon tetra-chloride. *J. Geophys. Res.*, **105**, 14 285–14 296.
- Waugh, D. W., T. M. Hall, and T. W. N. Haine, 2003: Relationships among tracer ages. *J. Geophys. Res.*, **108**, 3138, doi:10.1029/2002JC001325.
- , T. W. N. Haine, and T. M. Hall, 2004: Transport times and anthropogenic carbon in the subpolar North Atlantic Ocean. *Deep-Sea Res. I*, **51**, doi:10.1016/j.dsr.2004.06.011.